Tunnelling spin current and spin diode behaviour in a bilayer system

Pei-Qing Jin and You-Quan Li

Zhejiang Institute of Modern Physics and Department of Physics, Zhejiang University,
Hangzhou 310027, People's Republic of China

E-mail: pqjin@hbar.zju.edu.cn

Abstract
The coherent tunnelling spin current in the bilayer system with spin–orbit coupling is
investigated. Based on the continuity-like equations, we discuss the definition of the tunnelling
current and show that the overlaps between wavefunctions for different layers contribute to the
tunnelling current. We study the linear response of the tunnelling spin current to an in-plane
electric field in the presence of nonmagnetic impurities. The tunnelling spin conductivity we
obtained presents a feature asymmetrical with respect to the gate voltage when the strengths of
impurity potentials are different in each layer.

(Some figures in this article are in colour only in the electronic version)

1. Introduction

The study of the tunnelling process has a long history
ever since the foundation of quantum mechanics and
there arise many applicable effects. As an example,
the coherent tunnelling of Cooper pairs between weakly
connected superconductors, known as the Josephson effect,
has been employed in the design of superconductor circuits
that are prospective in quantum computation and quantum
information [1, 2]. For future information processing and
storage technologies, the emerging field of spintronics [3–5]
aims mainly at coherent manipulation of spin degree of
freedom and controllable spin transport in solid states. Owning
to these anticipations, some attention has been absorbed in
the study of the coherent spin tunnelling process either in
conventional Josephson junctions [6–8] or in the ferromagnetic
tunnel junctions [9]. However, as we are aware, the junction
constituted by a bilayer of two-dimensional electron gases
has not been considered yet although there exist versatile
features in such systems. For example, a resonantly enhanced
tunnelling was reported in the bilayer quantum Hall system
when the layers are sufficiently close to each other [10].
Moreover, the spin Hall conductivity, which vanishes for
arbitrarily small concentrations of nonmagnetic impurities in
a monolayer, was shown to have a magnification effect in
the bilayer electron system [11]. We therefore investigate the
coherent tunnelling spin current (TSC) in the bilayer system
with spin–orbit coupling in this paper. In our study, the

tunnelling is included in the unperturbed Hamiltonian, unlike
the conventional tunnelling Hamiltonian approach [12] where
it is treated as a perturbation.

The present paper is organized as follows. In section 2, we
revisit the definition of the tunnelling charge current and then
give the definition of the TSC with the help of the continuity-
like equations in bilayer systems. In section 3, we consider a
twin-layer system in which the strengths of impurity potentials
in each layer are identical. We study the linear response of
the TSC to the in-plane electric field and obtain the tunnelling
spin conductivity which exhibits sharp cusps. In section 4,
the influence on the tunnelling spin conductivity caused by
the variation of the strengths of impurity potentials in different
layers is considered. The expression of the Green's function
is extended so as to incorporate such influences. We find that
the difference between the strengths of impurity potentials in
the two layers gives rise to the asymmetrical feature of the
tunnelling spin current with respect to the gate voltage. Finally,
a brief summary is given in section 5 and some concrete
expressions are written out in the appendix.

2. Definition of coherent tunnelling spin current

In order to properly define the coherent TSC, let us first recall
the definition of the tunnelling charge current across a junction.
Such a current is generated by electrons tunnelling from one
side of the junction to the other side due to the imbalance of

the chemical potentials produced by an applied gate voltage V. The bilayer system considered in this paper resembles the tunnel junction and its Hamiltonian is given by

$$H = \frac{p^2}{2m} I + eV\tau_z + \beta\tau_x, \tag{1}$$

where β is the tunnelling strength, and I and τ_a ($a = x, y, z$) denote the unit matrix and Pauli matrices in the layer representation, respectively. The wavefunction of the system is expressed as $\Psi = (\psi_f, \psi_b)^T$. From the Schrödinger equation, we can obtain the continuity-like equations for the densities $\rho_\ell = \psi_\ell^\dagger \psi_\ell$, namely

$$\begin{aligned}
\frac{\partial \rho_f}{\partial t} + \frac{\partial j_{fi}}{\partial x_i} &= \frac{i\beta}{\hbar}(\psi_b^\dagger \psi_f - \text{h.c.}), \\
\frac{\partial \rho_b}{\partial t} + \frac{\partial j_{bi}}{\partial x_i} &= \frac{i\beta}{\hbar}(\psi_f^\dagger \psi_b - \text{h.c.}),
\end{aligned} \tag{2}$$

with $j_{\ell i} = -\frac{i\hbar}{2m}(\psi_\ell^\dagger \frac{\partial}{\partial x_i}\psi_\ell - \text{h.c.})$ and h.c. refers to the Hermitian conjugation since ψ_ℓ should be in a two-component form $\psi_\ell = (\psi_{\ell\uparrow}, \psi_{\ell\downarrow})^T$ if the spin degree of freedom is taken into account. Here the subscripts i represent the components of a quantity in the spatial space and ℓ label the quantities of the front layer with $\ell = f$ or the back layer with $\ell = b$. The nonvanishing terms on the right-hand sides of equations (2), which are caused by the tunnelling between layers, indicate the overlap between the wavefunctions for different layers.

Integrating the first equation of equations (2) over the domain of the front layer $\mathcal{D}_f$, we have

$$I_T = -\frac{dN_f}{dt} = \int j_{fz}\, dA - \frac{i\beta}{\hbar} \int_{\mathcal{D}_f} (\psi_b^\dagger \psi_f - \text{h.c.})\, dV, \tag{3}$$

where A denotes the area of the layer and $N_f = \int_{\mathcal{D}_f} \rho_f\, dV$ is the electron number in the front layer. Here we focus on the tunnelling-relevant direction, say the z direction, and assume that there is no in-plane current flowing out of each layer. Equation (3) demonstrates that the rate of change of the electron number in the front layer, defined as the tunnelling current, contains not only the conventional contribution $\int j_{fz}\, dA$, but also the overlap between the wavefunctions for different layers. The orthogonality and completeness of the states on each side of the junction were discussed [13–15]. Then equation (3) manifests, from another point of view, why the tunnelling current is conventionally evaluated by the rate of change of the electron number on one side of a junction.

Now we are in the position to consider the TSC in the bilayer system with spin–orbit coupling. A natural definition of the TSC density in a system should be the rate of change of the spin density $\vec{S}_\ell = \psi_\ell^\dagger \vec{s} \psi_\ell$ in the ℓ layer where $\vec{s} = \frac{\hbar}{2}\vec{\sigma}$ are the spin operators. Here and hereafter the overhead arrow represents that the quantity is a vector in the spin space. The continuity-like equations for the spin density $\vec{S}_\ell$ in the system with $SU(2)$ gauge potentials $\vec{\mathcal{A}}_0$ and $\vec{\mathcal{A}}_i$ [16] have been

obtained in our previous paper [11], which are

$$\begin{aligned}
&\left(\frac{\partial}{\partial t} - \hbar\vec{\mathcal{A}}_{f0}\times\right)\vec{S}_f + \left(\frac{\partial}{\partial x_i} + \hbar\vec{\mathcal{A}}_{fi}\times\right)\vec{J}_{fi} \\
&= \frac{i\beta}{\hbar}(\psi_b^\dagger \vec{s}\psi_f - \text{h.c.}), \\
&\left(\frac{\partial}{\partial t} - \hbar\vec{\mathcal{A}}_{b0}\times\right)\vec{S}_b + \left(\frac{\partial}{\partial x_i} + \hbar\vec{\mathcal{A}}_{bi}\times\right)\vec{J}_{bi} \\
&= \frac{i\beta}{\hbar}(\psi_f^\dagger \vec{s}\psi_b - \text{h.c.}),
\end{aligned} \tag{4}$$

with $\vec{J}_{\ell i} = \text{Re}(\psi_\ell^\dagger \frac{1}{2}\{v_i, \vec{s}\}\psi_\ell)$, where v_i is the velocity operator and the curly brackets denote the anti-commutation relation. In this paper, we consider the system without structure inversion symmetry and the resulting spin–orbit coupling is of Rashba type. In a single-layer electron gas it is given by $H_R = \alpha(k_y\sigma^x - k_x\sigma^y)$ [5]. Considering the strengths of the Rashba-type spin–orbit coupling may be different in the two layers, we employ α_1 and α_2 to denote the strengths in the front and back layers, respectively. Thus the Rashba-type spin–orbit coupling in a bilayer electron system is written as

$$H_R = \begin{pmatrix} \alpha_1 & 0 \\ 0 & \alpha_2 \end{pmatrix} \otimes (k_y\sigma^x - k_x\sigma^y) \tag{5}$$

and the $SU(2)$ gauge potentials are given by $\vec{\mathcal{A}}_{fx} = \frac{2m}{\hbar^2}(0, \alpha_1, 0)$, $\vec{\mathcal{A}}_{fy} = -\frac{2m}{\hbar^2}(\alpha_1, 0, 0)$, $\vec{\mathcal{A}}_{bx} = \frac{2m}{\hbar^2}(0, \alpha_2, 0)$, $\vec{\mathcal{A}}_{by} = -\frac{2m}{\hbar^2}(\alpha_2, 0, 0)$ and $\vec{\mathcal{A}}_{fz} = \vec{\mathcal{A}}_{f0} = \vec{\mathcal{A}}_{bz} = \vec{\mathcal{A}}_{b0} = 0$.

Since the tunnelling being considered is spin-independent, only a gate voltage cannot induce a nonvanishing TSC. As we know, an in-plane electric field is applied to drive the spin Hall current and the basic relation between the spin current J_i^a and the electric field is given by [17]

$$J_i^a = \epsilon_{aij}\sigma_s E_j, \tag{6}$$

where σ_s is the spin Hall conductivity and ϵ_{aij} the totally antisymmetric tensor. The indices i and a both run from 1 to 3 where i refers to the flowing direction of the spin current while a indicates the direction of the spin polarization. It demonstrates that the flow direction and the spin-polarization direction of the current as well as the direction of the electric field are always perpendicular to each other. Since the tunnelling is with respect to the z direction and the in-plane electric field is along the x direction, we focus on the component of the TSC polarized in the y direction. From equation (4), we have

$$-\frac{\partial S_f^y}{\partial t} = \left(\frac{\partial}{\partial z} + \hbar\mathcal{A}_{fy}^x\right)J_{fz}^y - \frac{i\beta}{\hbar}(\psi_b^\dagger s^y\psi_f - \text{h.c.}), \tag{7}$$

where we have taken that the nonvanishing components of the spin current are $J_{fz}^y = -J_{fy}^z$ as the electric field is along the x direction. The last term on the right-hand side of equation (7) can be regarded as the overlap between the eigenfunctions of s^y. Unlike the case of the tunnelling charge current, the contributions of the states with spin parallel and anti-parallel to the y axis have opposite signs. The covariant derivative $\frac{\partial}{\partial z} + \hbar\mathcal{A}_{fy}^x$ is in place of the conventional derivative, which indicates that the spin precession due to the spin–orbit coupling leads to an additional contribution to the TSC.

3. Tunnelling spin current in twin-layer system

In section 2, the definition of the TSC in bilayer systems with Rashba-type spin–orbit coupling in each layer has been discussed by taking account of the electrons' coherent tunnelling. Unlike the tunnelling Hamiltonian approach [12, 18] in the study of the tunnelling charge current, here we take the tunnelling term in the unperturbed Hamiltonian. Since the tunnelling strength is not necessarily weak in our approach, we are able to obtain more information beyond the perturbation approach. In the present approach, the unperturbed Hamiltonian in the second quantization form is given by

$$H = \sum_{\mathbf{k}} C_{\mathbf{k}}^{\dagger} \left\{ \begin{pmatrix} \frac{\hbar^2 k^2}{2m} + eV & \beta \\ \beta & \frac{\hbar^2 k^2}{2m} - eV \end{pmatrix} \otimes I \right.$$
$$\left. + \left(\alpha_+ I + \alpha_- \tau_z \right) \otimes (k_y \sigma^x - k_x \sigma^y) \right\} C_{\mathbf{k}} + \hat{V}_{\mathrm{im}}. \quad (8)$$

We have adopted the notations $\alpha_+ = (\alpha_1 + \alpha_2)/2$, $\alpha_- = (\alpha_1 - \alpha_2)/2$ and $C_{\mathbf{k}}^{\dagger} \equiv (c_{\mathbf{k},\mathrm{f}\uparrow}^{\dagger}, c_{\mathbf{k},\mathrm{f}\downarrow}^{\dagger}, c_{\mathbf{k},\mathrm{b}\uparrow}^{\dagger}, c_{\mathbf{k},\mathrm{b}\downarrow}^{\dagger})$ with $c_{\mathbf{k},\ell\uparrow(\downarrow)}^{\dagger}$ being the creation operator for a spin-up (spin-down) electron in the ℓ layer. Throughout the paper, the boldface of a quantity manifests that it is a two-dimensional vector, e.g. $\mathbf{k} = (k_x, k_y)$. The last term in the Hamiltonian characterizes the interaction between electrons and impurities. The influence of nonmagnetic [19–22] and magnetic [23, 24] impurities on the spin Hall conductivity were discussed in monolayer systems. For simplicity, we consider the nonmagnetic impurities in both layers are all alike in this section. Thus the potential energy of impurities is given by $\hat{V}_{\mathrm{im}} = u \sum_i \delta(\mathbf{r} - \mathbf{R}_i)$ with u being the strength and $\mathbf{R}_i$ the position of the impurity. Here we assume the interaction strength u is weak so that the Born approximation [25] is applicable.

In the chiral representation, the Hamiltonian without the impurity term is diagonalized by a unitary matrix U with eigenenergies

$$\varepsilon_1 = \epsilon_k - \alpha_+ k - \lambda_{12}, \qquad \varepsilon_2 = \epsilon_k - \alpha_+ k + \lambda_{12},$$
$$\varepsilon_3 = \epsilon_k + \alpha_+ k - \lambda_{34}, \qquad \varepsilon_4 = \epsilon_k + \alpha_+ k + \lambda_{34},$$

with $\epsilon_k = \frac{\hbar^2 k^2}{2m}$, $\lambda_{12} = \sqrt{(eV - \alpha_- k)^2 + \beta^2}$ and $\lambda_{34} = \sqrt{(eV + \alpha_- k)^2 + \beta^2}$. Hereafter, we set $\hbar = 1$ for simplicity. The free retarded Green's function in this chiral representation is given by $G_{0(\mathrm{ch})}^{\mathrm{R}}(\mathbf{k}, \omega) = \mathrm{diag}((\omega - \varepsilon_1 + i\eta)^{-1}, (\omega - \varepsilon_2 + i\eta)^{-1}, (\omega - \varepsilon_3 + i\eta)^{-1}, (\omega - \varepsilon_4 + i\eta)^{-1})$ with $i\eta$ being an infinitesimal quantity. Also the Green's function in the original representation is related to that in the chiral representation by the unitary transformation, namely $G(\mathbf{k}, \omega) = U(\mathbf{k}) G_{(\mathrm{ch})}(\mathbf{k}, \omega) U^{\dagger}(\mathbf{k})$.

As a macroscopic quantity, the TSC is expected not to be affected by the details of impurity location $\{\mathbf{R}_i\}$. We assume there is no correlation between impurities and employ the impurity averaging techniques and the diagrammatic method [25, 26]. A physical quantity Q for the whole system is obtained by taking the average over impurities' configuration, namely $\overline{Q} = \langle Q(\{\mathbf{R}_i\}) \rangle_{\mathrm{im}} = \Pi_i \int \frac{\mathrm{d}\mathbf{R}_i}{A} Q(\{\mathbf{R}_i\})$

with A being the size of the system. In the Born approximation, the averaged retarded Green's function $\overline{G^{\mathrm{R}}}(\mathbf{k}, \omega)$ satisfies the Dyson equation

$$\overline{G^{\mathrm{R}}}(\mathbf{k}, \omega) = G_0^{\mathrm{R}}(\mathbf{k}, \omega) + G_0^{\mathrm{R}}(\mathbf{k}, \omega)$$
$$\times \left(u n_{\mathrm{im}} + \frac{u^2 n_{\mathrm{im}}}{A} \sum_{\mathbf{q}} \overline{G^{\mathrm{R}}}(\mathbf{q}, \omega) \right) \overline{G^{\mathrm{R}}}(\mathbf{k}, \omega), \quad (9)$$

where n_{im} stands for the impurity concentration. The above equation has a self-consistent solution, $\overline{G_{(\mathrm{ch})}^{\mathrm{R}}}(\mathbf{k}, \omega) = \mathrm{diag}(g_1, g_2, g_3, g_4)$ with $g_j = (\omega - \varepsilon_j - u n_{\mathrm{im}} + \frac{i}{2\tau})^{-1}$, where the subscript j runs from 1 to 4. Here $\tau = (2\pi u^2 n_{\mathrm{im}} N_{\mathrm{F}})^{-1}$ is the momentum relaxation time and N_{F} is the density of states at the Fermi surface. Note that the averaged retarded Green's function is diagonal in the chiral representation. We will see in the next section that the difference between the strengths of impurity potentials in two layers results in the emergence of off-diagonal elements in $\overline{G_{(\mathrm{ch})}^{\mathrm{R}}}$.

The TSC defined in the previous section can be expressed in a symmetric form with respect to both layers, namely the difference between the rate of change of the spin operator in each layer:

$$J_z^y = -\frac{1}{2} \left\langle \frac{\mathrm{d}\hat{S}_-^y}{\mathrm{d}t} \right\rangle = -\frac{1}{2} \left\langle \frac{\mathrm{d}}{\mathrm{d}t} \sum_{\mathbf{k}} C_{\mathbf{k}}^{\dagger} (\tau_z \otimes s^y) C_{\mathbf{k}} \right\rangle, \quad (10)$$

where $\hat{S}_-^y = \hat{S}_{\mathrm{f}}^y - \hat{S}_{\mathrm{b}}^y$ denotes the difference between the y component of spin operators $\hat{S}_\ell^y = \sum_{\mathbf{k}} [(c_{\mathbf{k},\ell\uparrow}^{\dagger}, c_{\mathbf{k},\ell\downarrow}^{\dagger}) s^y (c_{\mathbf{k},\ell\uparrow}, c_{\mathbf{k},\ell\downarrow})^{\mathrm{T}}]$ in the two layers. It is written in a compact form in equation (10) where τ^z is in the layer representation. The linear response of the TSC to the external in-plane electric field, the tunnelling spin conductivity $\overline{\sigma^y}$, can be obtained by using the Kubo formula

$$\overline{\sigma^y}(\omega) = \frac{1}{2\pi\omega A} \int \mathrm{d}\omega_1 \mathrm{Tr} \left\{ n_{\mathrm{F}}(\omega_1) \right.$$
$$\times \overline{[G^{\mathrm{R}}(\omega_1) - G^{\mathrm{A}}(\omega_1)] \hat{j}_z^y G^{\mathrm{R}}(\omega + \omega_1) \hat{j}_e} + n_{\mathrm{F}}(\omega + \omega_1)$$
$$\left. \times \overline{[G^{\mathrm{R}}(\omega + \omega_1) - G^{\mathrm{A}}(\omega + \omega_1)] \hat{j}_e G^{\mathrm{A}}(\omega_1) \hat{j}_z^y} \right\}, \quad (11)$$

where $\hat{j}_z^y = \frac{1}{2}[(\alpha_+ \tau_z + \alpha_- I) \otimes k_y \sigma_z - \beta \tau_y \otimes \sigma_y]$ and Tr refers to the trace taken over the spin indices as well as the summation over the momentum. G^{A} is the advanced Green's function, n_{F} is the Fermi distribution function and $\hat{j}_e = e\hat{v}_x$ is the charge current operator.

In the uncrossing approximation [21], the dc tunnelling spin conductivity $\overline{\sigma^y}$ at zero temperature is calculated as the sum of contributions of the one-loop diagram $\overline{\sigma_0^y}$ and a series of ladder diagrams $\overline{\sigma_{\mathrm{L}}^y}$. The former is given by $\overline{\sigma_0^y} = -\frac{1}{2\pi A} \mathrm{Tr}(\overline{G^{\mathrm{R}}}(\mathbf{k}) \hat{j}_e(\mathbf{k}) \overline{G^{\mathrm{A}}}(\mathbf{k}) \hat{j}_z^y(\mathbf{k}))$ and denoted diagrammatically as

$$\overline{\sigma_0^y} = -\frac{1}{2\pi A} \hat{j}_z^y \quad \overline{G^{\mathrm{A}}} \quad \overline{G^{\mathrm{R}}} \quad \hat{j}_e.$$
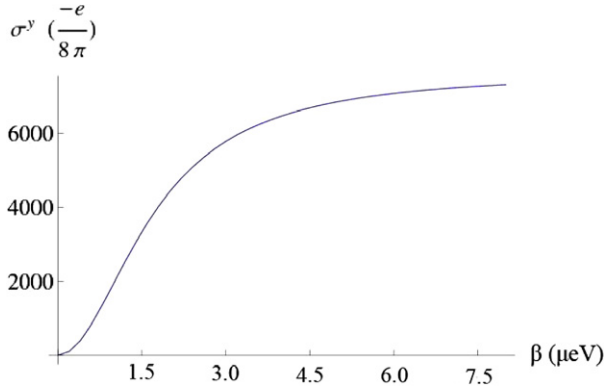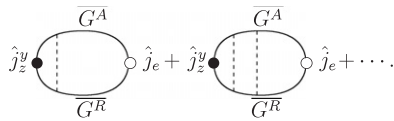
Figure 1. $\overline{\sigma^y}$ as a function of β. The parameters are given by $V = 0$, $\alpha_+ = 5.5 \times 10^{-14}$ eV m, $\alpha_- = 0.45 \times 10^{-14}$ eV m, $\mu = 0.1$ eV, $\tau = 660$ fs and the effective mass $m = 0.065\, m_0$ as in GaAs with m_0 being the mass of the free electron.

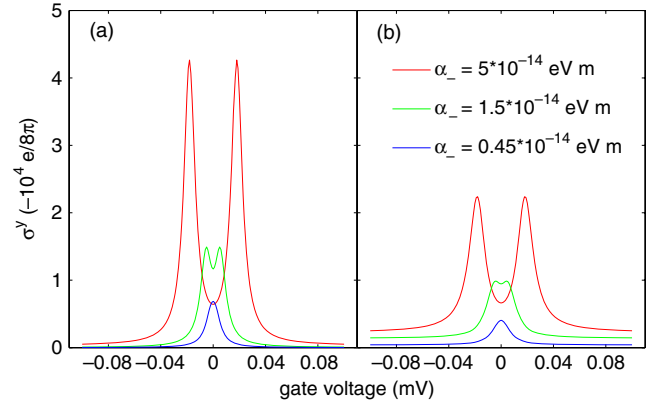**Figure 2.** Tunnelling spin conductivities $\overline{\sigma^y}$ are plotted as functions of the gate voltage V with different values of α_- given in the legend. The tunnelling strength is $\beta = 5 \times 10^{-6}$ eV, the momentum relaxation times are $\tau = 660$ fs in panel (a) and $\tau = 66$ fs in panel (b) while the other parameters are the same as those in figure 1.

A direct calculation leads to

$$\overline{\sigma_0^y} = -2\alpha_- \sum_{\mathbf{k}} \sin^2 \varphi$$

$$\times \text{Im}\Big[\frac{\beta^2}{\lambda_{12}} a_1 g_2 + \frac{\beta^2}{\lambda_{34}} a_3 g_4 + \alpha_+ k (a_1 + a_2)(g_3 + g_4)$$

$$+ W_{-+}(a_1 - a_2)(g_3 + g_4) + W_{+-}(a_1 + a_2)(g_3 - g_4)$$

$$+ W_{--}(a_1 - a_2)(g_3 - g_4) \Big], \tag{12}$$

where the simplified notations $W_{-+} = \frac{1}{2\lambda_{12}}(\beta^2 + (\alpha_+^2 + \alpha_-^2)k^2 - \frac{\alpha_+^2 + \alpha_-^2}{\alpha_-}keV)$, $W_{+-} = -\frac{1}{2\lambda_{34}}(\beta^2 + (\alpha_+^2 + \alpha_-^2)k^2 + \frac{\alpha_+^2 + \alpha_-^2}{\alpha_-}keV)$ and $W_{--} = \frac{\alpha_+ k}{\lambda_{12}\lambda_{34}}(e^2 V^2 - \beta^2 - \alpha_-^2 k^2)$ as well as the polar coordinates $\mathbf{k} = (k \cos \varphi, k \sin \varphi)$ are adopted. a_i are the matrix elements of the advanced Green's function in the chiral representation.

In the limit of a large Fermi circle, $\mu \gg \Delta_{ij}, 1/\tau$ with $\Delta_{ij} = \varepsilon_i - \varepsilon_j$, the vertex correction to the conductivity $\overline{\sigma_L^y}$ is dominated by the terms with one advanced and one retarded Green's function [21], which can be expressed diagrammatically as

$$\hat{j}_z^y \bullet \overset{\overline{G^A}}{\underset{\overline{G^R}}{\bigcirc}} \circ \hat{j}_e + \hat{j}_z^y \bullet \overset{\overline{G^A}}{\underset{\overline{G^R}}{\bigcirc}} \circ \hat{j}_e + \cdots.$$

The sum of vertex corrections to $\hat{j}_z^y$ can be defined as a new vertex $\mathcal{J}^y$, namely

$$\mathcal{J}^y \equiv \hat{j}_z^y \bullet \!\!\!\!\big< \; + \; \hat{j}_z^y \bullet \!\!\!\!\big< \; + \cdots.$$

Therefore $\overline{\sigma_L^y}$ can be written in a more compact form, i.e.

$$\overline{\sigma_L^y} = \frac{-1}{2\pi A} \text{Tr}(\overline{G^R}(\mathbf{k}) \hat{j}_e(\mathbf{k}) \overline{G^A}(\mathbf{k}) \mathcal{J}^y)$$

$$= -\frac{1}{2}\text{Im}\Big[\sum_{\mathbf{k}} \cos^2 \varphi \Big(\sum_{i,j=1}^{4} Q_{ij} a_i g_j$$

$$+ \sum_{s,s'=\pm 1} Q_{ss'}(a_1 + s\, a_2)(g_3 + s' g_4) \Big) \Big], \tag{13}$$

where the expressions for Q_{ij} and $Q_{ss'}$ are given in the appendix. The momentum-independent $\mathcal{J}^y$ can be obtained from the transfer matrix equation:

$$\mathcal{J}^y = \frac{u^2 n_{\text{im}}}{A} \sum_{\mathbf{q}} \overline{G^A}(\mathbf{q})(\hat{j}_z^y(\mathbf{q}) + \mathcal{J}^y)\overline{G^R}(\mathbf{q}). \tag{14}$$

The summation over the momentum can be evaluated by taking it as an integration in the limit of large Fermi circle. Then we obtain the tunnelling spin conductivity $\overline{\sigma^y}$ which is plotted as a function of β in figure 1. Here we consider the GaAs/AlGaAs double quantum well heterostructures [10]. We can see that the TSC vanishes when the tunnelling is absent.

We plot $\overline{\sigma^y}$ as a function of the applied gate voltage V with different α_- and momentum relaxation time in figure 2. It is shown that a peak in $\overline{\sigma^y}$ appears around $V = 0$ when α_- is small and this peak splits as α_- increases. These peaks manifest the resonance of the TSC. An intuitive interpretation is that the degeneracy of energies in different layers leads to a greatly enhanced tunnelling probability, as in the resonant tunnelling diode. We focus on the Fermi surface from which the main contribution to the current arises. The gate voltage induces a potential difference 2 eV between layers and the spin–orbit coupling causes an energy splitting between different spin states which equals $\Delta_f = \alpha_1 k_F$ in the front layer or $\Delta_b = \alpha_2 k_F$ in the back layer with k_F being the Fermi momentum, as shown in figure 3.

When α_- is small, $\Delta_f \simeq \Delta_b$ and the energies degenerate around $V = 0$ where there arises a peak in $\overline{\sigma^y}$. For large α_-, we first consider $V > 0$ and the energies degenerate when (a) $eV - \Delta_f = -eV + \Delta_b$ or (b) $eV - \Delta_f = -eV - \Delta_b$. However, only in situation (b) could the resonant tunnelling occur. It is due to the fact that the tunnelling in the system is spin-independent and the tunnelling between different spin states is forbidden. Thus the peak shows up at the degenerate point where $eV = \alpha_- k_F$, as shown in figure 2 ($k_F = 4 \times 10^8$ m^{-1} with the chosen parameters). Figures 3(c) and (d) show the two situations of energy degeneracy for $V < 0$. Similarly, only in situation (d) could a resonant TSC arise.
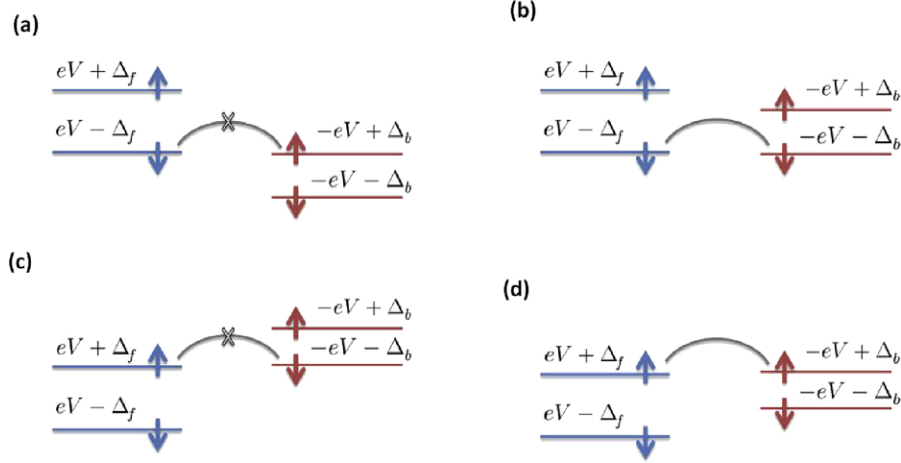
Figure 3. Energies of different spin states in the front (blue) and back (red) layers at the Fermi surface with $V > 0$ in panels (a) and (b) and $V < 0$ in (c) and (d). A resonance TSC shows up when the energies of states with the same spin direction in different layers degenerate.

The double-peak structure of $\overline{\sigma^y}$ in figure 2 demonstrates that the resonant TSC at $V > 0$ has the same sign as that at $V < 0$. It can be illustrated by a simple picture if we recall the definition of the TSC, i.e. the difference between the changing rates of the spin densities in different layers. Semiclassically, it can be expressed as $-\frac{1}{2}[(\frac{dn_f^\uparrow}{dt} - \frac{dn_f^\downarrow}{dt}) - (\frac{dn_b^\uparrow}{dt} - \frac{dn_b^\downarrow}{dt})]$ where $n_\ell^{\uparrow(\downarrow)}$ denotes the density of spin-up (spin-down) electrons in the ℓ layer. When $V > 0$, the potential energy of electrons in the front layer is higher and electrons tend to tunnel to the back layer, leading to $\frac{dn_f^\uparrow}{dt}, \frac{dn_f^\downarrow}{dt} < 0$ and $\frac{dn_b^\uparrow}{dt}, \frac{dn_b^\downarrow}{dt} > 0$. Furthermore, as presented in figure 3(b), the tunnelling probability of electrons with spin-down is much larger than that of electrons with spin up. Hence $|\frac{dn_\ell^\downarrow}{dt}| > |\frac{dn_\ell^\uparrow}{dt}|$ and the sign of the TSC is minus. The same result can be obtained for $V < 0$.

As expected, the nonmagnetic impurities tend to suppress the TSC, as indicated in figure 2(b) where the momentum relaxation time is a tenth part of that in figure 2(a). Figure 4 shows the contour-plot projections of $\overline{\sigma^y}$ which are plotted as a function of both the gate voltage and α_-. These figures indicate that the resonant peaks in $\overline{\sigma^y}$ begin to converge as α_- decreases.

4. Tunnelling spin current asymmetrical to gate voltage

In realistic samples, the strengths of impurity potentials in those two layers may not happen to be identical. We thus introduce u_f and u_b to denote the strengths of impurity potentials in the front and back layers, respectively. Accordingly, the interaction between electrons and impurities is given by

$$\hat{V}_{im} = \sum_i \delta(\mathbf{r} - \mathbf{R}_i) \begin{pmatrix} u_f & 0 \\ 0 & u_b \end{pmatrix} \otimes I. \quad (15)$$

Note that the unit matrix in the layer space is no longer appropriate in the present case. This implies that in the Feynman diagram the line which refers to the impurity
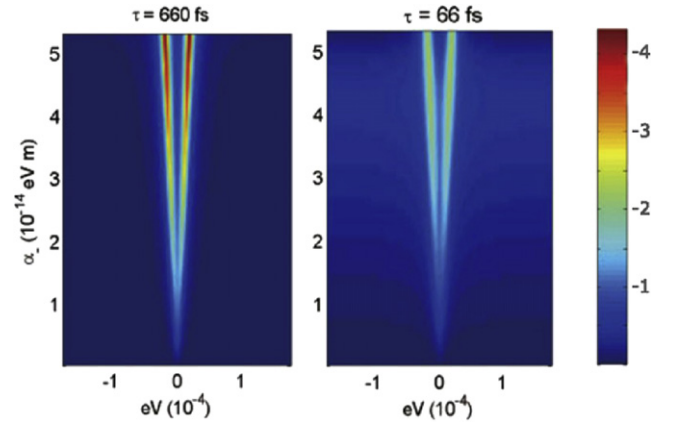

Figure 4. Contour plot of $\overline{\sigma^y}$ which is a function of both the gate voltage and α_-. The colour bar represents the value of $\overline{\sigma^y}$ in units of $10^4 e/8\pi$.

potential represents a matrix $\mathrm{diag}(u_f/A, u_b/A)$ rather than a number u/A. For example, the first-order Feynman diagram in the expansion of the impurity-averaged Green's function is given by

$$\underset{\mathbf{k}}{\overset{\times}{\cdots}} = N\, G_0(\mathbf{k}) \begin{pmatrix} \frac{u_f}{A} & 0 \\ 0 & \frac{u_b}{A} \end{pmatrix} G_0(\mathbf{k})$$

where the momentum is conserved at the vertex and the vector refers to the free Green's function. Accordingly, the Dyson equation for $\overline{G^R}$ is then written as

$$\overline{G^R}(\mathbf{k}, \omega) = G_0^R(\mathbf{k}, \omega) + G_0^R(\mathbf{k}, \omega) N \left[\begin{pmatrix} \frac{u_f}{A} & 0 \\ 0 & \frac{u_b}{A} \end{pmatrix} \right.$$
$$\left. + \sum_{\mathbf{q}} \begin{pmatrix} \frac{u_f}{A} & 0 \\ 0 & \frac{u_b}{A} \end{pmatrix} \overline{G^R}(\mathbf{q}, \omega) \begin{pmatrix} \frac{u_f}{A} & 0 \\ 0 & \frac{u_b}{A} \end{pmatrix} \right] \overline{G^R}(\mathbf{k}, \omega). \quad (16)$$

We obtain a self-consistent solution for the above equation:

$$\overline{G_{(ch)}^R} = \begin{pmatrix} R_{11} & R_+ & 0 & 0 \\ R_+ & R_{22} & 0 & 0 \\ 0 & 0 & R_{33} & R_- \\ 0 & 0 & R_- & R_{44} \end{pmatrix}, \quad (17)$$

5

with nonvanishing off-diagonal elements even in the chiral representation. The explicit expressions for those matrix elements are given in the appendix. The momentum relaxation time for the front and back layers are simply given by $\tau_f = (2\pi u_f^2 n_{im} N_F)^{-1}$ and $\tau_b = (2\pi u_b^2 n_{im} N_F)^{-1}$, respectively.

The difference between the strengths of impurity potentials in two layers not only modifies the diagonal elements of $\overline{G^R_{(ch)}}$ but also inevitably requires the appearance of off-diagonal elements. Now the contributions to $\overline{\sigma^y}$ by the diagonal elements can be directly obtained by replacing g_i and a_i, respectively, by R_{ii} and A_{ii} in equation (12) and equation (13). Here $A_{ii} = R_{ii}^*$ denote the diagonal elements of the averaged advanced Green's function in the chiral representation. The contributions to $\overline{\sigma_0^y}$ given by the off-diagonal elements are

$$
\overline{\sigma_{0,\text{off}}^y} = -2\beta \sum_{\mathbf{k}} \sin^2 \varphi \, \text{Im} \times \left[\left(R_+ \frac{eV\alpha_- + \alpha_+^2 k}{\lambda_{12}} \right. \right.
$$
$$
+ R_- \frac{\alpha_-(eV + \alpha_- k)}{\lambda_{34}} \bigg) (A_{33} + A_{44})
$$
$$
+ \left(R_+ \frac{k - \alpha_+ m}{m} - R_- \frac{\alpha_+ \lambda_{12}}{\lambda_{34}} \right) (A_{11} - A_{22})
$$
$$
- \left(R_+ \frac{\alpha_+ \lambda_{34}}{\lambda_{12}} + R_- \frac{k + \alpha_+ m}{m} \right) (A_{33} - A_{44})
$$
$$
+ \left(R_+ \frac{\alpha_-(eV - \alpha_- k)}{\lambda_{12}} + R_- \frac{eV\alpha_- - \alpha_+^2 k}{\lambda_{34}} \right)
$$
$$
\times (A_{11} + A_{22}) \bigg]. \tag{18}
$$

The transfer matrix equation for the vertex $\mathcal{J}^y$ is also modified as

$$
\mathcal{J}^y = N \sum_{\mathbf{q}} \begin{pmatrix} \frac{u_f}{A} & 0 \\ 0 & \frac{u_b}{A} \end{pmatrix} \overline{G^A}(\mathbf{q})(\hat{j}_z^y(\mathbf{q}) + \mathcal{J}^y)
$$
$$
\times \overline{G^R}(\mathbf{q}) \begin{pmatrix} \frac{u_f}{A} & 0 \\ 0 & \frac{u_b}{A} \end{pmatrix}. \tag{19}
$$

And the contributions to $\overline{\sigma_L^y}$ by the off-diagonal elements is

$$
\overline{\sigma_{L,\text{off}}^y} = -\text{Im} \left[\sum_{\mathbf{k}} \sum_{s,s'=+,-} \cos^2 \varphi \left(\sum_{i=1}^{4} X_{is} A_s R_{ii} + X_{ss'} A_s R_{s'} \right) \right], \tag{20}
$$

with $A_s = R_s^*$ and the coefficients X_{is} and $X_{ss'}$ are written out in the appendix.

The influence of the difference of impurity potentials on the tunnelling spin conductivity can be observed in figure 5. Here we introduce the difference in relaxation times $\Delta\tau = (\tau_f - \tau_b)/\tau_b$ which is taken to be 8×10^{-5} and 5×10^{-4} in figures 5(a) and (b), respectively. As the difference $\Delta\tau$ increases, the resonant peak located at $V > 0$ tends to be suppressed and finally it becomes a valley.

The impurity potentials can be viewed as a modification to the potential energy of electrons. As we have employed the impurity averaging techniques, the effective potential energies of electrons in the front and back layers are $eV + u_f$ and $-eV + u_b$, respectively. Also the potential difference between layers is given by $2eV + (u_f - u_b)$.
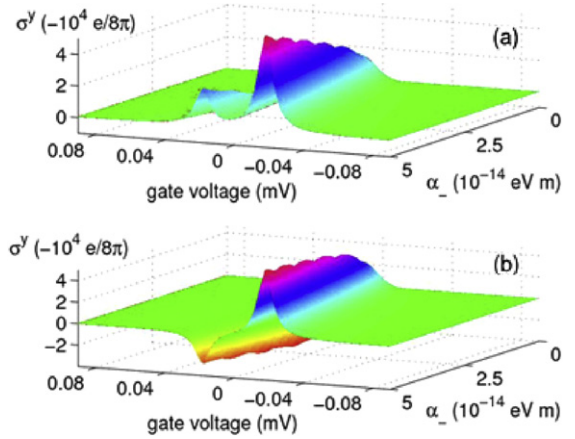

Figure 5. $\overline{\sigma^y}$ as a function of V and α_-. The relaxation-time differences are $\Delta\tau = 8 \times 10^{-5}$ in panel (a) and $\Delta\tau = 5 \times 10^{-4}$ in panel (b) with $\tau_b = 660$ fs.

When $V > 0$, the potential energy of the front layer is higher. Increasing $\Delta\tau$ reduces the potential difference between layers since $\tau_\ell \propto u_\ell^{-2}$ and $0 < u_f < u_b$. Finally the potential energy of the back layer becomes higher and electrons are inclined to tunnel from the back layer to the front layer. However, as the gate voltage $V > 0$, electrons in the spin-down states still have a larger tunnelling possibility. Hence the sign of the resulting resonant TSC is reversed and the peak in $\overline{\sigma^y}$ becomes a valley. When $V < 0$, electrons in the back layer are of higher potential energy. Increasing $\Delta\tau$ will not change this situation: it just increases the potential difference between layers. Therefore the resonant TSC still keeps its minus sign.

Figure 5 indicates that the variation of the strengths of impurity potentials between layers leads to the asymmetric dependence of the TSC on the gate voltage when the in-plane driven electric field is fixed. This unilateral conduction feature makes the bilayer system with different strengths of impurity potentials a candidate for the realization of a spin diode.

5. Summary

We have studied the coherent TSC in the bilayer system with spin–orbit coupling. We first revisited the definition of the tunnelling charge current with the help of continuity-like equations in the bilayer system since the tunnelling between layers causes the nonconservation of the density in each layer. In additional to the conventional contribution, the tunnelling current contains those related to the overlap of wavefunctions for different layers. This is intuitional for us to define the coherent TSC. We showed that the contributions of the wavefunction overlaps for states with spin parallel and anti-parallel to a reference axis have opposite signs. Unlike the conventional tunnelling Hamiltonian approach, the tunnelling strength in our study is not necessarily weak since it is treated as a part of the unperturbed Hamiltonian. In the light that only a gate voltage cannot induce a nonvanishing result, we studied TSC in response to an in-plane electric field. The spin conductivity was calculated in terms of the Kubo formula by taking account of nonmagnetic impurities. We firstly

investigated twin-layer systems and then considered the effect caused by the difference between the strengths of impurity potentials in different layers. Meanwhile, we developed the techniques dealing with the impurity-averaged Green's function in the bilayer system. We showed that there must exist nonvanishing off-diagonal elements in the averaged Green's function even in the chiral representation if the strengths of impurity potentials in two layers is different. Sharp cusps in the tunnelling spin conductivity appear near the null voltage and are suppressed by the impurities. We found that if the strength of impurity potential in one layer is different from that in the other layer, the TSC exhibits the asymmetrical feature with respect to the gate voltage. This reveals that the spin diode can also be realized in the bilayer system with different strengths of impurity potentials in different layers.

Acknowledgments

Appendix. Expressions for some coefficients and the matrices

The concrete expressions for the matrix elements of the averaged retarded Green's function in equation (17) is given by

$$
\begin{aligned}
R_{11} &= \left\{ \omega - \varepsilon_2 - w_+ - \frac{eV - \alpha_- k}{\lambda_{12}} w_- \right\} \\
&\times \{ (\omega - \varepsilon_1)(\omega - \varepsilon_2) - w_+(2\omega - \varepsilon_1 - \varepsilon_2) \\
&\quad + (\omega_+ + \omega_-)(\omega_+ - \omega_-) - 2\omega_-(eV - \alpha_- k) \}^{-1}, \\
R_{22} &= \left\{ \omega - \varepsilon_1 - w_+ + \frac{eV - \alpha_- k}{\lambda_{12}} w_- \right\} \\
&\times \{ (\omega - \varepsilon_1)(\omega - \varepsilon_2) - w_+(2\omega - \varepsilon_1 - \varepsilon_2) \\
&\quad + (\omega_+ + \omega_-)(\omega_+ - \omega_-) - 2\omega_-(eV - \alpha_- k) \}^{-1}, \\
R_{33} &= \left\{ \omega - \varepsilon_4 - w_+ - \frac{eV + \alpha_- k}{\lambda_{34}} w_- \right\} \\
&\times \{ (\omega - \varepsilon_3)(\omega - \varepsilon_4) - w_+(2\omega - \varepsilon_3 - \varepsilon_4) \\
&\quad + (\omega_+ + \omega_-)(\omega_+ - \omega_-) - 2\omega_-(eV + \alpha_- k) \}^{-1}, \\
R_{44} &= \left\{ \omega - \varepsilon_3 - w_+ + \frac{eV + \alpha_- k}{\lambda_{34}} w_- \right\} \\
&\times \{ (\omega - \varepsilon_3)(\omega - \varepsilon_4) - w_+(2\omega - \varepsilon_3 - \varepsilon_4) \\
&\quad + (\omega_+ + \omega_-)(\omega_+ - \omega_-) - 2\omega_-(eV + \alpha_- k) \}^{-1}, \\
R_+ &= \left\{ -\frac{\beta}{\lambda_{12}} w_- \right\} \\
&\times \{ (\omega - \varepsilon_1)(\omega - \varepsilon_2) - w_+(2\omega - \varepsilon_1 - \varepsilon_2) \\
&\quad + (\omega_+ + \omega_-)(\omega_+ - \omega_-) - 2\omega_-(eV - \alpha_- k) \}^{-1}, \\
R_- &= \left\{ -\frac{\beta}{\lambda_{34}} w_- \right\} \\
&\times \{ (\omega - \varepsilon_3)(\omega - \varepsilon_4) - w_+(2\omega - \varepsilon_3 - \varepsilon_4) \\
&\quad + (\omega_+ + \omega_-)(\omega_+ - \omega_-) - 2\omega_-(eV + \alpha_- k) \}^{-1},
\end{aligned}
$$

$$(A.1)$$

where we have introduced $w_\pm = \frac{1}{2}((u_f \pm u_b)n_{im} - \frac{i}{\tau_\pm})$ and $\tau_\pm = \frac{1}{2}(\tau_f - \tau_b)$.

The nonzero coefficients Q_{ij} in equation (13) are explicitly written as

$$
\begin{aligned}
Q_{11} &= \left(\frac{k}{m} - \alpha_2 + \alpha_- D_{12}^- \right) \\
&\times \left(D_{12}^- J_{12} - D_{12}^+ J_{34} + \frac{\beta}{\lambda_{12}}(J_{14} + J_{32}) \right), \\
Q_{22} &= -\left(\frac{k}{m} - \alpha_1 - \alpha_- D_{12}^- \right) \\
&\times \left(D_{12}^+ J_{12} - D_{12}^- J_{34} + \frac{\beta}{\lambda_{12}}(J_{14} + J_{32}) \right), \\
Q_{33} &= -\left(\frac{k}{m} + \alpha_2 - \alpha_- D_{34}^- \right) \\
&\times \left(D_{34}^+ J_{12} - D_{34}^- J_{34} + \frac{\beta}{\lambda_{34}}(J_{14} + J_{32}) \right), \\
Q_{44} &= \left(\frac{k}{m} + \alpha_1 + \alpha_- D_{34}^- \right) \\
&\times \left(D_{34}^- J_{12} - D_{34}^+ J_{34} + \frac{\beta}{\lambda_{34}}(J_{14} + J_{32}) \right), \\
Q_{12} &= \frac{2\alpha_- \beta}{\lambda_{12}} \left(\frac{\beta}{\lambda_{12}}(J_{12} - J_{34}) - D_{12}^- J_{14} - D_{12}^+ J_{32} \right), \\
Q_{34} &= \frac{2\alpha_- \beta}{\lambda_{34}} \left(\frac{\beta}{\lambda_{34}}(J_{12} - J_{34}) - D_{34}^- J_{14} - D_{34}^+ J_{32} \right),
\end{aligned}
$$

$$(A.2)$$

with $D_{12}^\pm = \frac{eV - \alpha_- k \pm \lambda_{12}}{\lambda_{12}}$, $D_{34}^\pm = \frac{eV + \alpha_- k \pm \lambda_{34}}{\lambda_{34}}$ and

$$
\begin{aligned}
Q_{+-} &= \frac{eV + \alpha_- k}{\lambda_{34}}(\alpha_2 J_{34} - \alpha_1 J_{12}) - \frac{\beta}{\lambda_{34}}(\alpha_1 J_{14} + \alpha_2 J_{32}), \\
Q_{-+} &= \frac{eV - \alpha_- k}{\lambda_{12}}(\alpha_2 J_{34} - \alpha_1 J_{12}) - \frac{\beta}{\lambda_{12}}(\alpha_2 J_{14} + \alpha_1 J_{32}), \\
Q_{++} &= (\alpha_1 J_{12} + \alpha_2 J_{34}), \\
Q_{--} &= \frac{1}{\lambda_{12}\lambda_{34}}[(\alpha_1 J_{12} + \alpha_2 J_{34}) \\
&\quad \times (e^2 V^2 - \alpha_-^2 k^2) + \beta^2(\alpha_2 J_{12} + \alpha_1 J_{34}) \\
&\quad + 2\alpha_- \beta(eV(J_{14} + J_{32}) - \alpha_+ k(J_{14} - J_{32}))],
\end{aligned}
$$

$$(A.3)$$

where $J_{12}, J_{14}, J_{32}, J_{34}$ are the matrix elements of the vertex $\mathcal{J}^y$ which can be obtained by solving equation (14).

The contribution to the $\overline{\sigma_L^y}$ by the off-diagonal elements of the Green's function is given by equation (20) and the coefficients therein are

$$
\begin{aligned}
X_{1+} &= \frac{\beta}{\lambda_{12}} \left(-\frac{k}{m} + \alpha_2 - 2\alpha_- D_{12}^- \right) J_{12} \\
&+ \frac{\beta}{\lambda_{12}} \left(\frac{k}{m} - \alpha_1 + 2\alpha_- D_{12}^+ \right) J_{34} \\
&+ \left(\frac{k}{m} D_{12}^+ + M_{12} - \alpha_- - \alpha_2 D_{12}^+ \right) J_{14} \\
&+ \left(\frac{k}{m} D_{12}^- + M_{12} - \alpha_- - \alpha_1 D_{12}^- \right) J_{32},
\end{aligned}
$$

$$X_{2+} = \frac{\beta}{\lambda_{12}} \left(-\frac{k}{m} + \alpha_2 + 2\alpha_- D_{12}^+ \right) J_{12}$$
$$+ \frac{\beta}{\lambda_{12}} \left(\frac{k}{m} - \alpha_1 - 2\alpha_- D_{12}^- \right) J_{34}$$
$$+ \left(\frac{k}{m} D_{12}^- - M_{12} + \alpha_- - \alpha_2 D_{12}^- \right) J_{14}$$
$$+ \left(\frac{k}{m} D_{12}^+ - M_{12} + \alpha_- - \alpha_1 D_{12}^+ \right) J_{32},$$

$$X_{3+} = \frac{\beta}{\lambda_{12}} \left(\alpha_2 - 2\alpha_- D_{34}^- \right) J_{12}$$
$$- \frac{\alpha_2}{\lambda_{12}} \left(eV - \alpha_- k + \frac{e^2 V^2 - \alpha_-^2 k^2}{\lambda_{34}} + \frac{\alpha_1 \beta^2}{\alpha_2 \lambda_{12}} \right) J_{14}$$
$$- \frac{\beta}{\lambda_{12}} \left(\alpha_2 - \frac{2\alpha_- (eV - \alpha_+ k)}{\lambda_{34}} \right) J_{34}$$
$$- \frac{\alpha_1}{\lambda_{34}} \left(eV - \alpha_- k - \frac{e^2 V^2 - \alpha_-^2 k^2}{\lambda_{34}} - \frac{\alpha_2 \beta^2}{\alpha_1 \lambda_{34}} \right) J_{32},$$

$$X_{4+} = \frac{\beta}{\lambda_{12}} \left(\alpha_2 + 2\alpha_- D_{34}^+ \right) J_{12}$$
$$- \frac{\alpha_2}{\lambda_{12}} \left(eV - \alpha_- k - \frac{e^2 V^2 - \alpha_-^2 k^2}{\lambda_{34}} - \frac{\alpha_1 \beta^2}{\alpha_2 \lambda_{12}} \right) J_{14}$$
$$- \frac{\beta}{\lambda_{12}} \left(\alpha_2 + \frac{2\alpha_- (eV - \alpha_+ k)}{\lambda_{34}} \right) J_{34}$$
$$- \frac{\alpha_1}{\lambda_{34}} \left(eV - \alpha_- k + \frac{e^2 V^2 - \alpha_-^2 k^2}{\lambda_{34}} + \frac{\alpha_2 \beta^2}{\alpha_1 \lambda_{34}} \right) J_{32},$$

$$X_{1-} = \frac{\beta}{\lambda_{34}} \left(\alpha_2 - 2\alpha_- D_{12}^- \right) J_{12}$$
$$- \frac{\alpha_2}{\lambda_{34}} \left(eV + \alpha_- k - \frac{\alpha_1 (e^2 V^2 - \alpha_-^2 k^2)}{\alpha_2 \lambda_{12}} - \frac{\beta^2}{\lambda_{12}} \right) J_{14}$$
$$- \frac{\beta}{\lambda_{34}} \left(\alpha_2 - \frac{2\alpha_- (eV + \alpha_+ k)}{\lambda_{12}} \right) J_{34}$$
$$- \frac{\alpha_1}{\lambda_{34}} \left(eV + \alpha_- k + \frac{\alpha_2 (e^2 V^2 - \alpha_-^2 k^2)}{\alpha_1 \lambda_{12}} + \frac{\beta^2}{\lambda_{12}} \right) J_{32},$$

$$X_{2-} = \frac{\beta}{\lambda_{34}} \left(\alpha_2 + 2\alpha_- D_{12}^+ \right) J_{12}$$
$$- \frac{\alpha_2}{\lambda_{34}} \left(eV + \alpha_- k + \frac{\alpha_1 (e^2 V^2 - \alpha_-^2 k^2)}{\alpha_2 \lambda_{12}} + \frac{\beta^2}{\lambda_{12}} \right) J_{14}$$
$$- \frac{\beta}{\lambda_{34}} \left(\alpha_2 + \frac{2\alpha_- (eV + \alpha_+ k)}{\lambda_{12}} \right) J_{34}$$
$$- \frac{\alpha_1}{\lambda_{34}} \left(eV + \alpha_- k - \frac{\alpha_2 (e^2 V^2 - \alpha_-^2 k^2)}{\alpha_1 \lambda_{12}} - \frac{\beta^2}{\lambda_{12}} \right) J_{32},$$

$$X_{3-} = \frac{\beta}{\lambda_{34}} \left(\frac{k}{m} + \alpha_2 - 2\alpha_- D_{34}^- \right) J_{12}$$
$$- \frac{\beta}{\lambda_{34}} \left(\frac{k}{m} + \alpha_1 - 2\alpha_- D_{34}^+ \right) J_{34}$$
$$- \left(\frac{k}{m} D_{34}^+ - M_{34} + \alpha_- + \alpha_2 D_{34}^+ \right) J_{14}$$
$$- \left(\frac{k}{m} D_{34}^- - M_{34} + \alpha_- + \alpha_1 D_{34}^- \right) J_{32},$$

$$X_{4-} = \frac{\beta}{\lambda_{34}} \left(\frac{k}{m} + \alpha_2 + 2\alpha_- D_{34}^+ \right) J_{12}$$
$$- \frac{\beta}{\lambda_{34}} \left(\frac{k}{m} + \alpha_1 + 2\alpha_- D_{34}^- \right) J_{34}$$
$$- \left(\frac{k}{m} D_{34}^- + M_{34} - \alpha_- + \alpha_2 D_{34}^- \right) J_{14}$$
$$- \left(\frac{k}{m} D_{34}^+ + M_{34} - \alpha_- + \alpha_1 D_{34}^+ \right) J_{32},$$

$$X_{++} = M_{12} (J_{12} - J_{34}) + \left(\frac{k}{m} - \alpha_+ \right) (J_{12} + J_{34})$$
$$+ \frac{2\beta\alpha_- (eV - \alpha_- k)}{\lambda_{12}^2} (J_{14} + J_{32}),$$

$$X_{--} = M_{34} (J_{12} - J_{34}) - \left(\frac{k}{m} + \alpha_+ \right) (J_{12} + J_{34})$$
$$+ \frac{2\beta\alpha_- (eV + \alpha_- k)}{\lambda_{34}^2} (J_{14} + J_{32}),$$

$$X_{+-} = \frac{2}{\lambda_{12}\lambda_{34}} \Big(\left(\alpha_2 \left(e^2 V^2 - \alpha_-^2 k^2 \right) + \alpha_1 \beta^2 \right) J_{12}$$
$$+ \left(\alpha_1 \left(e^2 V^2 - \alpha_-^2 k^2 \right) + \alpha_2 \beta^2 \right) J_{34}$$
$$- 2\beta\alpha_- \left((eV + \alpha_+ k) J_{14} + (eV - \alpha_+ k) J_{32} \right) \Big),$$

$$(A.4)$$

and $X_{-+} = 0$ with $M_{12} = \frac{\alpha_-}{\lambda_{12}^2}(eV + \beta - \alpha_- k)(eV - \beta - \alpha_- k)$
and $M_{34} = \frac{\alpha_-}{\lambda_{34}^2}(eV + \beta + \alpha_- k)(eV - \beta + \alpha_- k)$.

References

[1] Fitzgerald R 2002 *Phys. Today* **55** (6) 14
[2] You J Q and Nori F 2005 *Phys. Today* **58** (11) 42
[3] D'yakonov M I and Perel' V I 1971 *JETP Lett.* **13** 467
[4] Wolf S A, Awschalom D D, Buhrman R A and Daughton J M 2001 *Science* **294** 1488
[5] Zutic I, Fabian J and Dassarma S 2004 *Rev. Mod. Phys.* **76** 323
[6] Choi M S, Bruder C and Loss D 2000 *Phys. Rev.* B **62** 13569
[7] Grønsleth M S, Linder J, Børven J M and Sudbø A 2006 *Phys. Rev. Lett.* **97** 147002
[8] Zhao E H and Sauls J A 2007 *Phys. Rev. Lett.* **98** 206601
[9] Lee Y L and Lee Y W 2003 *Phys. Rev.* B **68** 184413
[10] Spielman I B, Eisenstein J P, Pfeiffer L N and West K W 2000 *Phys. Rev. Lett.* **84** 5808
[11] Jin P Q and Li Y Q 2007 *Phys. Rev.* B **76** 235311
[12] Cohen M H, Falicov L M and Phillips J C 1962 *Phys. Rev. Lett.* **8** 316
[13] Prange R E 1963 *Phys. Rev.* **131** 1083
[14] Zawadowski A 1967 *Phys. Rev.* **163** 341
[15] Caroli C, Combescot R and Lederer D 1975 *Phys. Rev.* B **12** 3977
[16] Jin P Q, Li Y Q and Zhang F C 2006 *J. Phys. A: Math. Gen.* **39** 7115
     Jin P Q and Li Y Q 2008 *Phys. Rev.* B **77** 155304
[17] Murakami S, Nagaosa N and Zhang S C 2003 *Science* **301** 1348
     Sinova J, Culcer D, Niu Q, Sinitsyn N A, Jungwirth T and MacDonald A H 2004 *Phys. Rev. Lett.* **92** 126603
[18] Mahan G D 2000 *Many-Particle Physics* (New York: Plenum) p 788
[19] Inoue J I, Bauer G E W and Molenkamp L W 2003 *Phys. Rev.* B **67** 033104

Inoue J I, Bauer G E W and Molenkamp L W 2004 *Phys. Rev. B* **70** 041303

[20] Mishchenko E G, Shytov A V and Halperin B I 2004 *Phys. Rev. Lett.* **93** 226602

[21] Dimitrova O V 2005 *Phys. Rev. B* **71** 245327

[22] Engel H A, Rashba E I and Halperin B I 2006 *Handbook of Magnetism and Advanced Magnetic Materials* vol V (New York: Wiley)

[23] Inoue J I, Kato T, Ishikawa Y, Itoh H, Bauer G E W and Molenkamp L W 2006 *Phys. Rev. Lett.* **97** 046604

[24] Wang P, Li Y Q and Zhao X 2007 *Phys. Rev. B* **75** 075326

[25] Haug H and Jauho A P 1996 *Quantum Kinetics in Transport and Optics of Semiconductors* (Berlin: Springer) p 51

[26] Abrikosov A A, Gorkov L P and Dzyaloshinski I E 1975 *Methods of Quantum Field Theory in Statistical Physics* (New York: Dover)